

Rapid time variations of water maser emission in W3(OH) and NGC 6334C

Y. Xu^{1,2}, X.W. Zheng³, F.J. Zhang^{1,2}, Z.Y. Yu^{1,2}, P. Han^{2,4}, E. Scalise Jr.⁵, and Y.J. Chen^{1,2}

¹ The Chinese Academy of Sciences, Shanghai Astronomical Observatory, Shanghai 200030, P.R. China

² The Chinese Academy of Sciences, Chinese National Observatories, Beijing 100080, P.R. China

³ Nanjing University, Department of Astronomy, Nanjing 210093, P.R. China

⁴ Purple Mountain Observatory, Nanjing 210008, P.R. China

⁵ Department of Astrophysics, INPE, Brazil

Received 27 September 1999 / Accepted 10 July 2000

Abstract. We report the observed results of a short time scale monitoring of the 22 GHz water maser emission in W3(OH) and NGC 6334C. Both sources were monitored daily for about a month. The aim of the observations is to investigate the possible presence of very short interval variations on time scales of hours or days. Our observations showed that the flux density of the component at -52.8 km s^{-1} in W3(OH) decayed linearly with a timescale of about 19 days, and a maser in NGC 6334C flared rapidly, doubling the flux with a timescale of about 4 days. The rapid time variability of the observed water maser features may be caused by an external pumping event. The collision among dense clumps at sufficient relative velocities supplies the powerful energy required to excite H₂O maser emission and then quenches the pump in the following days or longer period.

Key words: masers – stars: formation – ISM: individual objects: NGC 6334F – ISM: individual objects: W3(OH)

1. Introduction

Interstellar masers are generally found in star-forming regions and are excellent signposts for both the low-mass and massive star formation. Observations have shown that most interstellar water masers are associated with the youngest objects, which usually have strong outflows. The flux density varies on time scales ranging from a few days to several months. The maser variability in certain sources is extraordinary. Detailed investigation enables us to understand not only the masers, but the relationship between the masers and their exciting centers.

W3(OH) region, at a distance of 2.2 pc (Humphreys 1978), contains at least two sites within a projected distance of 0.1 pc, in which massive stars are forming or have newly formed. Radio and IR observations indicate that the most prominent site is the ultra-compact HII region in the $1''.3$ size, consisting of a 3 Jy radio continuum source and OH and CH₃OH masers (Reid et al. 1995). The OH maser spots are projected against the optically thick radio continuum source associated O star. Situated $\sim 6''$,

or ~ 0.06 pc, to the east of the radio continuum source is a complex of strong H₂O masers (Dreher & Welch 1981). The H₂O masers are too far from the HII region to be excited by the O star. The presence of hot, dense HCN at the H₂O position indicates a possible second source of luminosity (Turner & Welch 1984). A H₂O flare was detected in the masing region by Haschick et al. (1977). The flux density of the feature rose for a time period of eight days and then decayed slowly over the following month. The flux density of some components reached more than 2000 Jy (Sullivan 1973; Moran et al. 1973; Little et al. 1977; Genzel et al. 1978). Based on VLBI observations, the relative proper motions of the H₂O masers in the region outlined a bipolar outflow (Alcolea et al. 1993). The center of expansion appeared to be coincident with a dense, compact molecular clump detected in HCN emission (Turner & Welch 1984) and a nonthermal radio continuum emission (Reid et al. 1995).

NGC6334, at a distance of 1.74 kpc (Neckel 1978), is the largest and the most complex region of active star formation known in the Galaxy. The complex consists of three large HII region. Based on radio and IR observation, there are a large number of compact sources (Reid & Moran 1981; dePree et al. 1995; Tapia et al. 1996) in the region, such as active centers probably in different evolutionary stages and bipolar molecular outflows. NGC6334 has a variety of indicators of active star formation such as hot CO spots, far-infrared peaks, OH and H₂O masers. Five sites of H₂O masers have been found in the complex (Moran & Rodriguez 1980). Among them, NGC 6334C is peculiar because it has a large blueshift, $\sim 80 \text{ km s}^{-1}$, while the other four masers all have velocity centroids within 10 km s^{-1} of the cloud velocity. Moreover, the maser emission from NGC 6334C is two orders of magnitude more luminous than the other four masers. The spectacular water masers showed many features, in which seven main components had flux densities of more than 150 Jy, and the peak flux was about 1000 Jy. Because the ultra-compact HII region near NGC 6334C is optically thick at 4.9 GHz, the associated star has been inferred earlier than O 9.5 (Rodriguez et al. 1980).

With the objective of studying very short-time scale (days or hours) variations of the water maser emission at 22 GHz, a

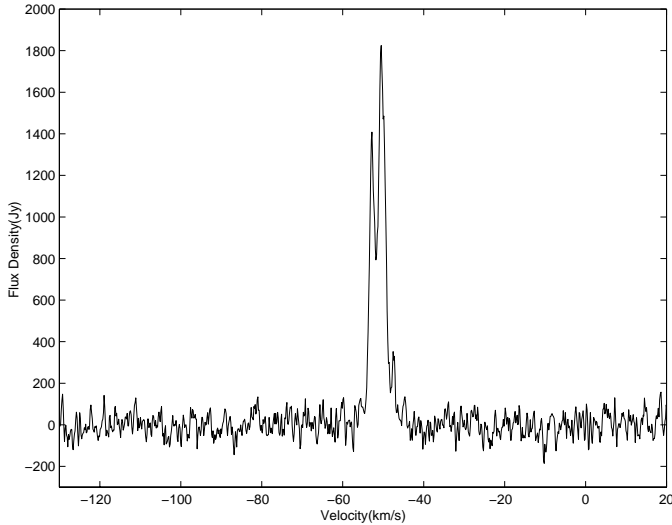


Fig. 1. Water maser spectra in W3(OH). The velocity resolution is 0.163 km/s.

monitoring program of 14 sources was undertaken using the 13.7 m radio telescope in the Purple Mountain Observatory. Here we present the monitoring results of the water maser emission from W3(OH) and NGC 6334C.

2. Observations and results

The observations were carried out from August 25 through September 24, 1993 using the 13.7 m telescope at the Qinghai Station of Purple Mountain Observatory. This antenna is located in the Gobi desert, a very dry and arid region at 3200 m above sea level in western China. It is a classic Cassegrain telescope and has a pointing accuracy better than $20''$ and a HPBW $4'.2$ at 22 GHz. It is front-end operated with a cooled schottky mixer and a 1.4 GHz FET IF amplifier. The system temperature is about 1500 K. The local oscillator is a phase locked Gunn diode. A high resolution 1024 channels AOS is employed as a back-end. We checked the AOS performance daily during our observations. The measurements suggested that the AOS operated with an average channel separation of 12.10 ± 0.02 kHz and a frequency resolution of 22.1 ± 1.8 kHz (Zheng & Lei 1998).

Observations were made in position-switching mode and a 120 K noise diode was used as a second calibrator. To check the stability of the noise diode a number of continuum sources were observed. During the period of observations the weather conditions at the site were excellent. The atmospheric opacity was about 0.05 in the zenith direction. The telescope sensitivity was 38 Jy K^{-1} , and the absolute calibration for flux density was about 20%.

In order to eliminate any gain dependence effect of the radio telescope all the observations were carried out at the same sidereal time, i.e. at the same parallactic angle and elevation angles. To discriminate between the instrumental effects and the real changes in the flux density the monitoring program included 14 sources selected with different spectral features. The spectrum of W3(OH) water maser emission shows three components at

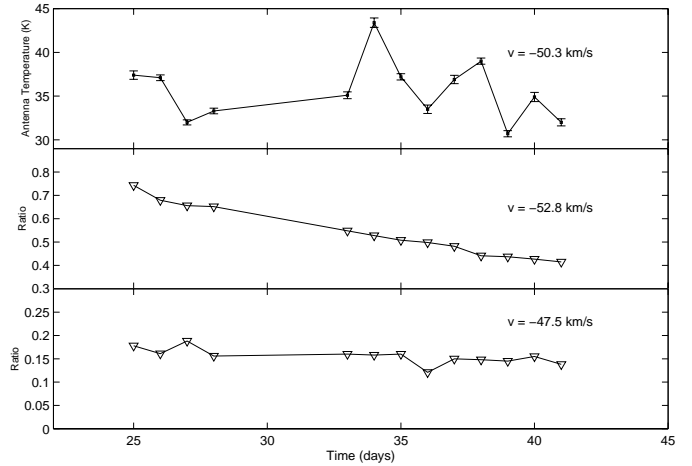


Fig. 2. Radio light curves of three components in W3(OH). In the top panel, the time variability of the reference feature appears to be caused by the instrumental effects. In the middle and bottom panels, we show the relative intensity variations of components at $V_{LSR} = -47.5$ and -52.8 km s^{-1} . The monitoring observations were carried out from August 25 through September 24, 1993. The time axes on the figure show days since August 1, 1993.

$V_{LSR} = -47.5, -50.3$ and -52.8 km s^{-1} (see Fig. 1). The rms noise level (1σ) in the plot is about 1.0 K, obtained in 240 s integration. The peak antenna temperature, the radial velocity, the linewidth and the line area for each component was fitted by a one-dimensional Gaussian model. In order to eliminate the effects of uncalibrated gain fluctuations, the strongest component at $V_{LSR} = -50.3 \text{ km s}^{-1}$ was selected as a reference feature. The light curve of the reference feature and amplitude ratio curves to the reference feature for the other two components are plotted in Fig. 2. The -50.3 km s^{-1} component was the most intense of the three components during the whole observing period, and its peak intensity was about 1830 Jy (see Fig. 1). The flux density of the -52.8 km s^{-1} component decayed linearly, and was still decreasing when our observations ceased. The period for the feature to reach half the initial intensity was about 19 days. The flux density of the component at -47.5 km s^{-1} showed no significant variations or, if there was any variation, it was of the same order of magnitude as the rms value. The time-variations of the W3(OH) spectra are displayed in Fig. 3 for selected scans. The time variability of the -52.8 km s^{-1} component is apparent.

In Fig. 4 the relation between the flux density, F , and the line width, ΔV , of the -52.8 km s^{-1} component is plotted. The data were fitted by a straight line $\Delta V \propto F^{-0.44 \pm 0.10}$. This relationship is very close to the results obtained by Mattila et al. (1985).

The spectrum of the water maser emission in the NGC 6334C region, shown in Fig. 5, manifests three water components at $-81.2, -84.4$ and -86.8 km s^{-1} . The other two bumps in the line wing may result from the combination of these three components. As mentioned above, the strongest component at $V_{LSR} = -81.2 \text{ km s}^{-1}$ was selected as a reference feature. Ratios of amplitude to the reference feature for two other components

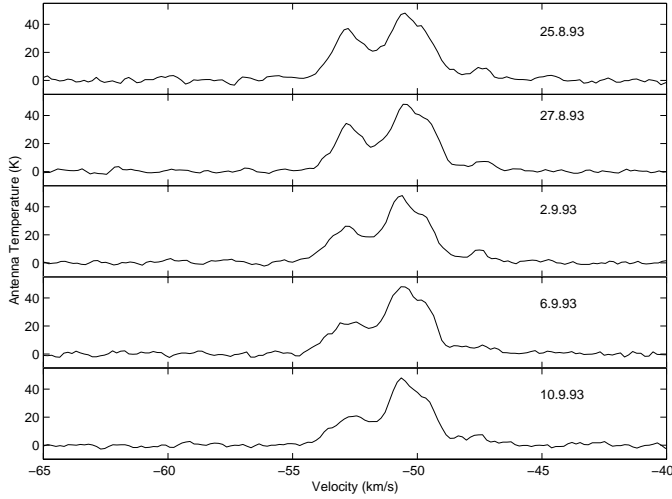


Fig. 3. Time-variations of the W3(OH) water maser spectra during the period of our observations.

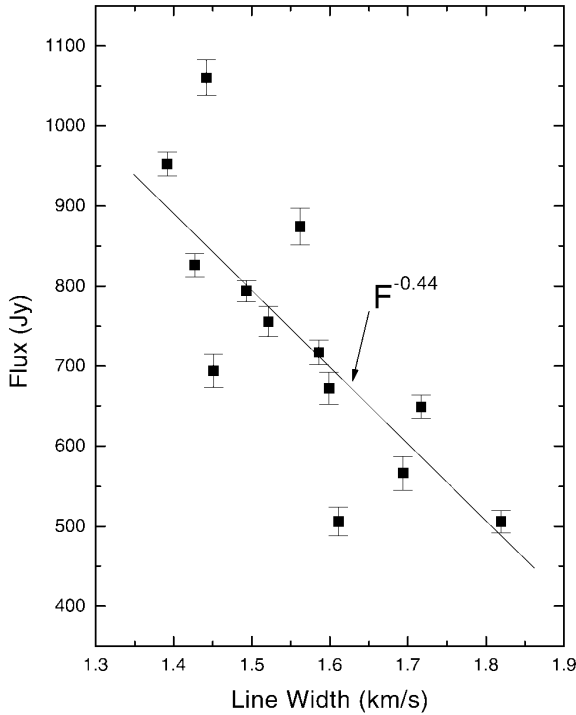


Fig. 4. The relationship between the flux density, F , and the linewidth, ΔV , for the -52.8 km s^{-1} component in W3(OH). The straight line describes the relation $\Delta V \propto F^{-0.44}$.

as well as the light curve of the peak component are plotted in Fig. 6.

After a phase of slow climbing of about 15 days, the flux density of the -84.4 km s^{-1} component jumped from 1090 to 2200 Jy. The timescale was about 4 days. We found that the event happened in all three components (see Fig. 6). Unfortunately, we did not have continuous records of an hour or shorter time interval for the source. Therefore, a positive assessment for instrumental effects or intrinsic changes may not be determined completely. If the event in these components is true, one

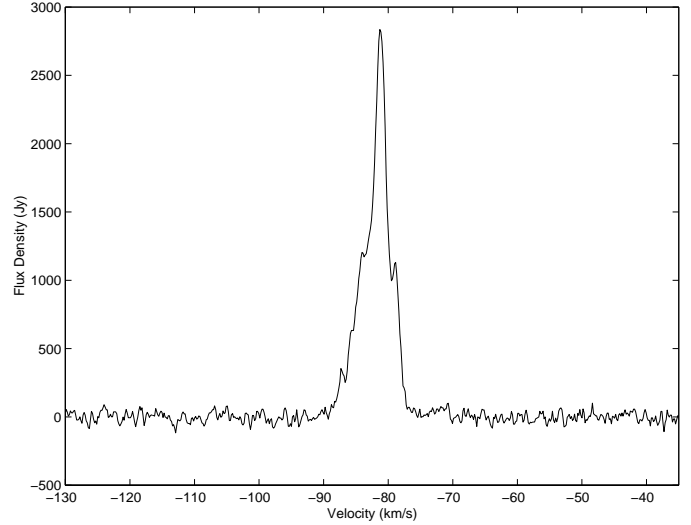


Fig. 5. Water maser spectra in NGC 6334C. The velocity resolution is 0.163 km/s .

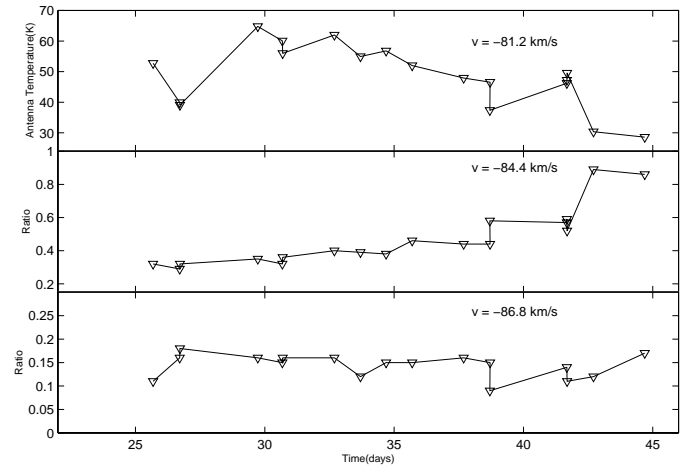


Fig. 6. Radio light curves of three components in NGC 6334C. The top panel shows the time variability of the reference feature. In the middle and bottom panels, we show the relative intensity variations of components at $V_{LSR} = -84.4$ and -86.8 km s^{-1} .

alternative explanation is an external pumping event, such as clump-clump collision, which will be discussed in detail below. The external event affects the three components simultaneously, but with different degrees of impact. The time-variations of the maser source are displayed in Fig. 7.

3. Discussion

In order to interpret reasonably the rapid time variability, the physical parameters in the masing region should be obtained. The brightness temperature of maser emission can be expressed as (Moran 1989)

$$T_B = \frac{c^2}{2k\nu^2} \frac{F}{\Omega_s}, \quad (1)$$

where c is the speed of light, and k is Boltzmann's constant. $\Omega_s \sim \pi a^2/D^2$ is the apparent angular size of the source as

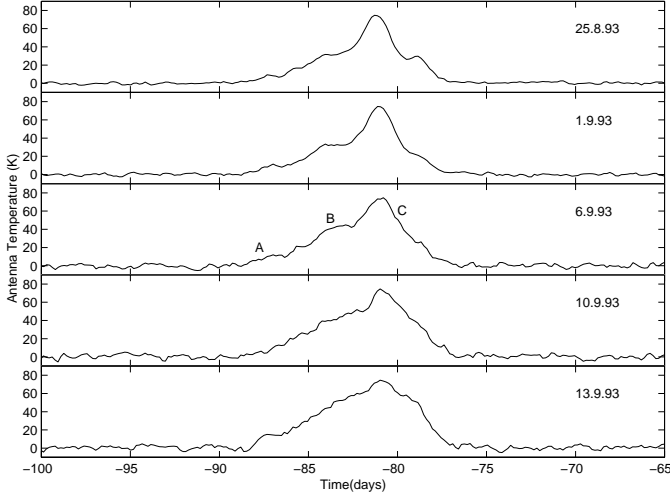


Fig. 7. Time-variations of the NGC 6334C water maser spectra during the period of our observations.

seen by the observer and a is the radius of maser spots which have the typical size of 10^{13} cm (Reid & Moran 1981). F and ν are the measured flux density at line center and observing frequency, respectively. The initial flux density of the -84.4 km s^{-1} component in NGC 6334C was about 750 Jy. Eq. (1) indicates T_B to be about $3.2 \cdot 10^{12}$ K. Similarly, for the -52.8 km s^{-1} component in W3(OH), its lowest flux density was 685 Jy. It implies $T_B = 4.6 \cdot 10^{12}$ K. The total population in the 6_{16} and 5_{23} levels for the saturated water maser can be expressed as (Moran 1989)

$$n_{12} = \frac{8}{h\nu} A^{3/4} (\Gamma\eta)^{-7/4} \frac{\Delta\nu}{D} \theta_s^{-3} F, \quad (2)$$

where $\Delta\nu$ and θ_s are the maser linewidths and observed source sizes. η is the pump efficiency, usually assumed to be 0.01, and A and Γ are the Einstein coefficients and the decay rate per molecule from the maser levels, respectively. For the 22 GHz H_2O transition, $A = 1.9 \cdot 10^9 s^{-1}$, and Γ is expected to be $\sim 1 s^{-1}$. The total gas density, which is predominately molecular hydrogen, n_{H_2} can be estimated for an H_2O maser by the equation (Moran 1989)

$$n_{H_2} = n_{12} \frac{n_{H_2O}}{n_{12}} \frac{n_{H_2}}{n_{H_2O}}, \quad (3)$$

where n_{H_2O} is the density of water molecules. For masers associated with star-forming regions, $n_{H_2O}/n_{12} \sim 10^2$, and $n_{H_2}/n_{H_2O} \sim 10^4$, therefore, the hydrogen density, n_{H_2} , was decreasing from about 2.0 to $1.1 \cdot 10^8 cm^{-3}$ for the -52.8 km s^{-1} component in W3(OH) and increasing from about 0.8 to $2.4 \cdot 10^8 cm^{-3}$ for the -84.4 km s^{-1} component in NGC 6334C during our observations. In masing regions, changes in the density of gas can give rise to an effective change in pump rate. Interstellar H_2O masers are too far from the central star to be radiatively pumped (Moran 1989). Kylafis & Norman (1991) discussed the pumping of H_2O masers in star-forming regions by collisions with H_2 molecules. According to their view, the number density of H_2 molecules derived above is too low to produce such a high brightness temperature (10^{12} K).

Burke et al. (1978) studied an H_2O maser flare in W3(OH) and obtained a good fit using a simple model in which energy was released very quickly inside a spherical maser cloud. This model could not work appropriately in our experiment, because it did not account for flickering behavior observed during the rise of the -81.2 km s^{-1} flare in NGC 6334C and also did not explain why the flux density of the -52.8 km s^{-1} component in W3(OH) decayed almost linearly unless the feature was undergoing an exponential decay, but was far down on the tail of the curve.

The rapid time variability of the observed water maser features could arise from a radiative instability of masers, interstellar scintillation and changes in the pump rate.

In partially saturated masers, a radiative instability can cause a periodic variation, but most of the models focus on OH masers with timescales of the order of hours (Scappaticci & Watson 1992).

The rapid time variations could also be due to interstellar propagation effects, such as diffractive or refractive scintillation. For the strongly diffractive scintillation, the correlation timescale is $t_d \sim \lambda/2\pi\theta_s v_t$ for a source of angular size θ_s , observing wavelength λ , and a relative transverse velocity v_t (Simonetti et al. 1993). For water masers in W3(OH), the typical diameter of maser spot $d_s \simeq 1 \cdot 10^{13}$ cm and $v_t \simeq 20$ km s^{-1} (Alcolea et al. 1993), the diffractive timescale is about 50 s. The correlation timescale of refractive scintillation is $t_r \sim d_0/v_t$, where d_0 is the observed angular size. For the assumption $d_0 = d_s$, the refractive timescale is about 90 days. Obviously, the former is too short compared to our observing timescale while the latter is somewhat long. However, the true sizes of the water masers in the two regions are likely to be less than the typical estimate in diameter, and the refractive time scale might fit the fluctuation time observed in our experiment.

All water maser sources in both W3(OH) and NGC 6334C are located near ultra-compact HII regions. At the initial phases of star formation, a strong stellar wind is one of the main characteristics. This extremely fast wind, moving at velocities of several hundred km s^{-1} , may very well drive the molecular outflows. As the result of the influence of the energetic protostellar wind, the dense clumps are dispersed into space. Clumps either create shocks in the surrounding clouds or are themselves shock compressed. Masers within the compressed gas, with beamings perhaps perpendicular the clump's motions. Their motions and superposition of their beamings may cause the variabilities of the masers. The variabilities of the observed masers require random gas movements of ≥ 50 km s^{-1} which are unreasonably large (Mattila et al. 1985).

Tarter & Welch (1986) suggested that if collisions take place among clumps at sufficient relative velocities, the powerful energy can excite H_2O maser emission. The collision rapidly heats the gas to the temperature of the dust and thus quenches the pump. Because the energy is associated with the relative velocity v , the model requires a wide range of collision velocities among dense clumps. In order to obtain v , in the present paper, we assume that both collision clouds are the same. Some physical parameters in the masing region are $F \sim 2000$ Jy, $D \sim 2$ kpc, and $\Delta\nu \sim 50$ kHz and the total luminosity of the maser,

$L = 4\pi D^2 \Delta\nu \sim 5 \cdot 10^{29} \text{ erg s}^{-1}$. The apparent isotropic maser luminosity, L_m (for a spherical maser, $L_m = L$), is given by the equation (Moran 1989)

$$L_m = \frac{4\pi \nu_m}{\Omega_0 \nu_p} \eta L_k, \quad (4)$$

where L_k is the rate of dissipation of kinetic energy, and ν_m and ν_p are the frequency of maser and pump frequency, respectively. If the pump operates at $\sim 40 \mu\text{m}$, then $L_k \sim 2 \cdot 10^{29} \text{ erg s}^{-1}$. According to Reid & Moran (1988) and Tarter & Welch (1986)

$$L_k = \frac{\pi}{2} r^2 n_a m_{H_2} v^3, \quad (5)$$

where r , n_a and m_{H_2} are the size of the maser cloud, the number density of gas in the maser cloud, and the mass of a hydrogen molecule, respectively. In the present paper, $r \sim 4 \cdot 10^{14} \text{ cm}$, and $n_a \sim 10^8 \text{ cm}^{-3}$, hence, we obtain $v \sim 10 \text{ km s}^{-1}$. VLBI observations indicated that the magnitude of proper motions of some masers in the W3(OH) region was quite different from that of other masers in the region. This implies that there was a wide range of velocities among dense clumps. Similarly, the large blue shift of the water masers in NGC 6334C suggests there were strong activities in the masing region, indicating a possible existence of a wide range of velocities among dense clumps. So, the relative velocity $v \sim 10 \text{ km s}^{-1}$ is common among these maser clouds. The collision among maser clouds naturally provides a explanation for the rapid time variations.

4. Conclusion

Daily monitoring for a period of about a month has allowed accurate measurements of rapid variations of the water masers in W3(OH) and NGC 6334C and the results can be summarized as follows:

The flux density of the -52.8 km s^{-1} component in W3(OH) decayed linearly with the timescale of 19 days, and the -84.4 km s^{-1} component in NGC 6334C flared rapidly, rising from 1090 to 2200 Jy with a timescale of about 4 days.

The rapid time variations could be explained by interstellar propagation effects, but even if the true size of the water source in NGC 6334C has an order of magnitude less than the typical estimate in diameter, the refractive time scale was still hard to fit to the fluctuation time scale seen in NGC 6334C.

The collision rapidly heats the gas to the temperature of the dust and thus quenches the pump in the following few days or

longer period. The collision may cause the rapid time variabilities of the observed water maser features.

Acknowledgements. We wish to thank the referee, J.M.Moran, for a critical reading of the manuscript and very useful comments. We thank D.R.Jiang for valuable discussions. Xu is grateful to the staff of the Laboratory for Astronomical Data Analysis and Computational Physics in Nanjing university for their assistance during his visit.

References

- Alcolea J., Menten K.M., Moran J.M., Reid M.J., 1993, In: Clegg A.W., Nedoluha G.E. (eds.) *Astrophysical Masers*. Springer-Verlag, Heidelberg, p. 225
- Burke B.F., Giuffrida T.S., Haschick A.D., 1978, *ApJ* 226, L21
- dePree C.G.D., Rodriguez L.F., Dickel H.R., Goss W.M., 1995, *ApJ* 447, 220
- Dreher J.W., Welch W.J., 1981, *ApJ* 245, 857
- Genzel R., Downes D., Moran J.M., et al., 1978, *A&A* 66, 13
- Haschick A.D., Burke B.F., Spencere J.H., 1977, *Sci* 198, 1153
- Humphreys R.H., 1978, *ApJS* 38, 309
- Kylafis N.D., Norman C., 1991, *ApJ* 373, 525
- Little L.T., White G.J., Riley P.W., 1977, *MNRAS* 180, 639
- Mattila K., Holsti N., Toriseva M., et al., 1985, *A&A* 145, 192
- Moran J.M., 1989, In: Harquist T.W. (ed.) *Molecular Astrophysics. A Volume Honoring Alexander Dalgarno*. Cambridge University Press, p. 397
- Moran J.M., Papadopoulos G.D., Burke B.F., et al., 1973, *ApJ* 185, 535
- Moran J.M., Rodriguez L.F., 1980, *ApJ* 236, L159
- Neckel T., 1978, *A&A* 69, 51
- Reid M.J., Argon A.L., Masson C.R., Menten K.M., Moran J.M., 1995, *ApJ* 443, 238
- Reid M.J., Moran J.M., 1981, *ARA&A* 19, 231
- Reid M.J., Moran J.M., 1988, In: Verschuur G.L., Kellermann (eds.) *Galactic and Extragalactic Radioastronomy*. 2nd ed. Springer, New York, ch. 6
- Rodriguez L.F., Moran J.M., Ho P.T.P., Gottlieb E.W., 1980, *ApJ* 235, 845
- Scappaticci G.A., Watson W.D., 1992, *ApJ* 400, 351
- Simonetti J.H., Diamond P.J., Uphoff J.A., Boboltz D., Dennission B., 1993, In: Clegg A.W., Nedoluha G.E. (eds.) *Astrophysical Masers*. Springer, Heidelberg, p. 311
- Sullivan W.T., 1973, *ApJS* 25, 393
- Tarter J.C., Welch W.J., 1986, *ApJ* 305, 467
- Tapia M., Persi P., Roth M., 1996, *A&A* 316, 102
- Turner J.L., Welch W.J., 1984, *ApJ* 287, L81
- Zheng X., Lei C., 1998, *Chin. Astro. Astrophysics* 22, 244